

Experimental Evaluation of a Vision-based Measuring Device for Parallel Machine-tool Calibration

Pierre Renaud¹, Nicolas Andreff¹, Michel Dhome², Philippe Martinet²

¹LaRAMA, U. Blaise Pascal/IFMA, Clermont-Ferrand, France, renaud/andreff@ifma.fr

²LASMEA, U. Blaise Pascal/CNRS, Clermont-Ferrand, France, dhome/martinet@lasmea.univ-bpclermont.fr

Abstract

In this article, evaluation of a vision-based measuring system for parallel machine-tool calibration is performed. The simultaneous measurement of the 6 pose components enables one to perform calibration using the efficient inverse kinematic method. The system is composed of a single camera and a calibration board generated on a LCD monitor. Calibration board size can be adapted to the camera field of view, and specific points of interest can be generated, in order to improve pose measurement. Based on a single industrial camera, the measuring system is low-cost and easy-to-use. An experimental evaluation of the system is performed on a machine-tool axis. Measurement bias and precision are estimated by comparison with laser interferometry, and influence of focal length and sensor resolution is examined.

1 Introduction

Machine-tools with parallel structure fulfill the requirements of High Speed Machining (HSM) [5, 4]. The use of such structures for machining is however dependent on the ability to produce mechanisms with accuracy in the order of $1\mu m$. A kinematic calibration is therefore needed, *i.e.* enhancing the machine-tool accuracy by determining the actual values which describe the geometrical dimensions of the structure [2]. Among the proposed calibration methods [22, 15, 7], Inverse Kinematic Model (IKM) algorithm seems to be the most efficient [8]. According to it, accuracy enhancement is achieved by minimizing the error committed on proprioceptive sensor estimation, which necessitates an external pose measurement, *i.e.* measurement of the 6 degrees of freedom (d.o.f.) defining position and orientation of the tool in the machine coordinate frame. The measuring system for parallel machine-tool calibration has to perform such measurement, which accuracy in the order of $1\mu m$, 1° in a $500 \times 500 \times 500mm^3$ volume. As a whole set of pose measurements must be performed, the measuring procedure should be fast and

easy to use.

Some adapted measuring systems have been proposed in the literature. One theodolite, with two measuring tapes [19], or two theodolites [14] enables one to measure the 3D position of a point by triangulation. The measure is accurate but the cost of automated systems is very high [16]. Laser tracking systems, based on interferometry, allow one to perform accurate 3D measurement in the previously specified volume [1, 21]. The cost of such measuring systems is nevertheless also very high and they may be complex to use [17]. For the two previous measuring systems, each pose estimation must furthermore be computed based on the sequential 3D position measurement of several points. Specific mechanical devices have been designed to measure accurately the pose of a solid [11, 6]. Micrometer measurement accuracy can be achieved, however these measuring systems seem to have reduced measurement volume.

On the opposite, with vision-based measurement systems, one can measure the pose of the camera w.r.t the calibration block [10]. Its use for parallel structure calibration is therefore of particular interest [25]. Measurement volume is only limited by the observation of the calibration block. Due to the use of standard industrial cameras, such systems remain low-cost, around one tenth of a laser interferometer. However, the main difficulty is to get a high ratio measurement accuracy/measurement volume.

In this paper, we propose to perform parallel machine-tool calibration with a vision-based measuring system. This system is composed of a single CCD camera and calibration boards displayed on a LCD monitor. An experimental evaluation of the measuring system for calibration is achieved by simultaneous measurements on a HSM machine-tool axis with the vision-based system and 1D laser interferometry. In the first part of this document, the need for a full-pose measuring system is justified. The measuring principle and system set-up are then presented, and in the third part, the method used to analyze experimentally measurement bias is detailed. Exper-

imental results are then presented, analyzing precision and trueness of the measuring system. Influence of the CCD sensor resolution and optics is examined. Conclusions about the evaluated specifications of the measuring system and developments are then finally given.

2 Calibration using Inverse Kinematic Model

The IKM expresses the controlled joint variables q as a function of the end-effector pose L :

$$q = f(L, \xi) \quad (1)$$

where ξ is the geometrical parameter vector. To identify this vector ξ , an error function is minimized, which compares estimated variables $q_{est} = f(L, \xi)$ and the measured ones \tilde{q} for N different positions [24]:

$$\min_{\xi} \sum_{i=1}^N \|f(L_i, \xi) - \tilde{q}_i\|^2 \quad (2)$$

Identification of the actual values describing the geometrical dimensions of the structure can be achieved by minimizing this error function. The use of an analytical model avoids numerical problems that may occur with methods using direct kinematic model [8]. Furthermore, for some structures like Stewart platforms, identification can be achieved by considering each leg of the structure, hence reducing the number of parameters to identify simultaneously [23]. Identification can be performed in the whole workspace, contrary to methods based on mechanical constraints [15, 7], increasing the identification accuracy.

For calibration methods using the direct kinematic model, the error function can be modified to take into account the performed measurements of the end-effector pose [3]. With IKM calibration method, the whole pose of the end-effector must be measured. The proposed measuring system is therefore well designed for this context.

3 Description of the Measuring System

3.1 Set-up

The measuring system is composed of a CCD camera (Figure 1), fixed on the moving part, and a calibration board, composed of several dots. The calibration board is generated using a LCD monitor (Figure 2).

3.2 From Image to the Pose

The image is supposed to respect the pin-hole model [12]. Recall that the image coordinates (x, y) of a point are bound to its coordinates (X, Y, Z) in the calibration board frame by:

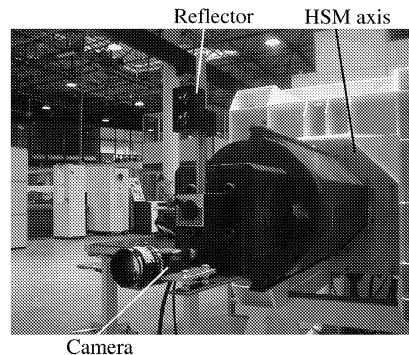


Figure 1: Camera and reflector on a HSM axis.

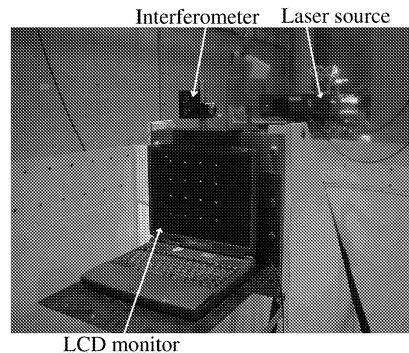


Figure 2: Interferometer, LCD monitor and laser source.

$$s \cdot \begin{pmatrix} x \\ y \\ 1 \end{pmatrix} = \begin{pmatrix} KR & Kt \end{pmatrix} \cdot \begin{pmatrix} X \\ Y \\ Z \\ 1 \end{pmatrix} \quad (3)$$

with $L = (R, t)$ the pose to determine, K the intrinsic parameters of the camera. This projection equation is only defined to an arbitrary factor s . The intrinsic parameters related to this model, including optical distortions, are determined during the calibration of the measuring system. A sequence of about 8 images is necessary to calibrate simultaneously the camera and the calibration board [18]. The pose L is determined by non-linear optimization [9].

3.3 Screen-displayed Calibration Boards

Measurement accuracy is bound to the quality of determination of the dot centers and to the sensitivity of the optimisation process to the components of the pose L .

The determination of the dot centers is achieved by identifying gray-level variations in the image with the contour of the dots. By using calibration boards gen-

erated with the LCD monitor, the geometry of the dots and the gray-level variations can be precisely defined in order to ensure a more accurate localization of the dot centers than with physical calibration blocks.

Pose estimation accuracy increases with the size of the calibration board image. However, the calibration board has to stay in the field of view of the camera for any measurement configuration. In order to meet these two requirements, several calibration boards, with different sizes, are generated on the LCD monitor. For each camera position, the largest visible calibration board i is used to determine the pose L_i , which defines the transformation from the calibration board coordinate frame R_{Mi} to the camera coordinate frame R_C . The set of calibration boards is generated with a common coordinate frame, which enables one to express finally all the pose measurements in a single coordinate frame. The ratio measurement volume/accuracy can therefore be increased by the use of screen-displayed calibration boards.

4 Measuring System Evaluation

The measuring system evaluation is achieved by conducting simultaneous measurements with the vision-based system and a laser interferometer on a HSM machine-tool axis. It consists in estimating trueness, expressed in terms of bias, and precision. Trueness is the closeness of agreement between the average value obtained from a large series of test results and an accepted reference value and precision the closeness of agreement between independent test results obtained under stipulated conditions [13].

4.1 Laser Interferometer Measurement Principle

The laser interferometer set-up consists of a laser source and 2 optics : an interferometer (Figure 2) and a reflector (Figure 1). A single degree of freedom is measured for each laser interferometer configuration, defined by the mounted optics. Only a differential measure is provided: an initial pose has to be arbitrarily defined in order to express the measured displacement. Nevertheless, optics have to be modified to access to the different degrees of freedom. Measurements are therefore not expressed in a common coordinate frame.

4.2 Measurement Coordinate Frames

The laser interferometer measures some of the components of ${}^{Om}T_{Of}$, the transformation from R_{Om} , the reflector coordinate frame, to R_{Of} , the interferometer coordinate frame (figure 3). The vision-based system measures ${}^C T_M$, the transformation from the

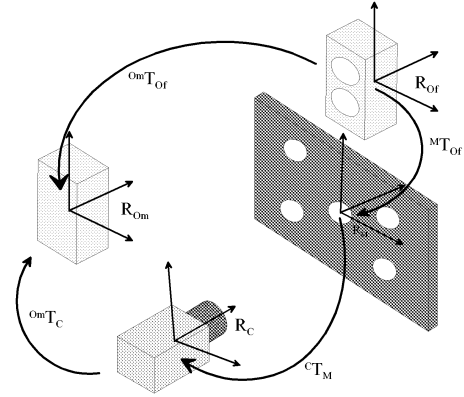


Figure 3: Measurement coordinate frames and associated transformations.

camera coordinate frame R_C to the calibration board frame R_M . During each experimentation, the calibration board and the interferometer are rigidly linked and their relative position can be defined by ${}^M T_{Of}$, transformation between their respective coordinate frames. In the same way, the reflector and the camera are rigidly linked and their relative position defined by the transformation ${}^{Om}T_C$. Notice that interferometric and vision-based measurements are not expressed in the same coordinate frames.

4.3 Precision Estimation

The evaluation of the measuring system consists in determining measurement trueness and precision. Pose measurements, achieved for different axis positions, include the axis behavior and measurement errors. Consecutive positions are chosen close enough so that the pose difference can be considered only due to the measurement error. The measurement standard deviation is then computed from the set of pose differences in the calibration board coordinate frame.

4.4 Trueness Estimation

The trueness estimation is achieved considering interferometric measures to be reference values. For comparison sake only, vision-based measures have to be expressed in the interferometer coordinate frame. For each axis position i , the transformation between the interferometer and reflector frames can be expressed as a function of the vision-based measurement:

$${}^{Om}T_{Of}^i = {}^{Om}T_C {}^C T_M^i {}^M T_{Of} \quad (4)$$

As interferometric measures are differential, equation (4) is expressed between two consecutive measurement positions i and $i + 1$:

$${}^{Om}T_{Of}^i ({}^{Om}T_{Of}^{i+1})^{-1} = {}^{Om}T_C {}^C T_M^i ({}^C T_M^{i+1})^{-1} ({}^{Om}T_C)^{-1} \quad (5)$$

The measurement coordinate frames are positioned such that frame orientations are almost identical. The angles characterizing the previously defined transformations remain therefore to a small amplitude, and (5) can be linearized:

$$\left\{ \begin{array}{l} \Delta\alpha_{OmOf} = \Delta\alpha_{CM} \\ \Delta\beta_{OmOf} = \Delta\beta_{CM} \\ \Delta\gamma_{OmOf} = \Delta\gamma_{CM} \\ \Delta x_{OmOf} = -\Delta\gamma_{CM} \cdot y_{MOF} + \Delta\beta_{CM} \cdot z_{MOF} \\ \quad + \Delta x_{CM} - \gamma_{OmC} \cdot \Delta y_{CM} + \beta_{OmC} \cdot \Delta z_{CM} \\ \Delta y_{OmOf} = \Delta\gamma_{CM} \cdot x_{MOF} - \Delta\alpha_{CM} \cdot z_{MOF} \\ \quad + \gamma_{OmC} \cdot \Delta x_{CM} + \Delta y_{CM} - \alpha_{OmC} \cdot \Delta z_{CM} \\ \Delta z_{OmOf} = -\Delta\beta_{CM} \cdot x_{MOF} + \Delta\alpha_{CM} \cdot y_{MOF} \\ \quad - \beta_{OmC} \cdot \Delta x_{CM} + \alpha_{OmC} \cdot \Delta y_{CM} + \Delta z_{CM} \end{array} \right. \quad (6)$$

Thus, the angular variations are directly comparable. However, 6 parameters related to the experimental set-up ($x_{MOF}, y_{MOF}, z_{MOF}, \alpha_{OmC}, \beta_{OmC}, \gamma_{OmC}$) have to be estimated in order to compare the translation displacement measures. As these parameters interfere linearly in (6), a least-squares estimation can be computed. Estimation bias is reduced by performing parallel filtering of the linear system [20].

Due to the use of the laser interferometer, measurement path has to be linear. This exciting trajectory [16] is too weak to allow the identification of the 6 parameters. For each interferometer measurement configuration, only two parameters can be identified, and the other parameter *a priori* values are employed. Bias analysis is consequently rather delicate.

5 Experimental Results

5.1 Experimental Set-up

The HSM machine-tool axis stroke is equal to $400mm$. A Renishaw ML10 interferometer is employed, with a fixed interferometer (Figure 2) and a moving reflector (Figure 1). Three measuring system set-ups were experimented in order to evaluate the influence of the calibration board size, focal length and sensor resolution. In the first case, the camera has a resolution of 768×576 pixels, 8bit-encoded with a $50mm$ lens. For the second set-up, the same camera is equipped with an $8mm$ lens. For the third set-up, the camera has a resolution of 1024×768 pixels, 8bit-encoded with a $6mm$ lens. Images are stored on a PC via a video capture board. Calibration boards are displayed on a $14''$ LCD screen, with a 1024×768 pixels resolution. The axis displacement between two measurements is equal to $5mm$. For each position, 10 images are stored and their average value is considered for the pose evaluation, in order to reduce high-frequency noise. The axis displacement direction z corresponds roughly to the camera axis.

Table 1: Estimated standard-deviations.

D.o.f	Set-up 1	Set-up 2	Set-up 3
R_x	0.105°	$1.8E-3^\circ$	$1.5E-3^\circ$
R_y	0.110°	$1.5E-3^\circ$	$1.6E-3^\circ$
R_z	$1.4E-3^\circ$	$1.8E-3^\circ$	$1.0E-3^\circ$
T_x	$3.17\mu m$	$3.98\mu m$	$2.6\mu m$
T_y	$3.98\mu m$	$4.53\mu m$	$3.0\mu m$
T_z	$135\mu m$	$18\mu m$	$12\mu m$

5.2 Precision

First measurement set-up. With a $50mm$ lens, the calibration board image size is almost constant during the axis displacement. First measurements were then achieved using a single calibration board, to minimize influence of image size. The measuring system precision is higher for displacement measurements along x and y axis and rotation around the z axis (Table 1 - Set-up 1). This behavior is bound to the measuring principle and the measurement configuration: displacements in the calibration board plane are directly perceptible in the camera image, contrary to displacements orthogonal to the board plane.

Influence of the Calibration Board Size. A second calibration board, observable for $0 < z < 200mm$, is computed to quantify the influence of the calibration board size. A significant decrease of the estimated standard deviations is observed: precision is increased by about 45% for a size modification of 60%. Hence, the interest of multiple screen-displayed calibration boards is confirmed.

Influence of the Focal Length. For the second set-up, the image size variation is higher, with a smaller calibration board image for $z = 0$. The measuring precision is however significantly higher (Table 1 - Set-up 2). This precision increase is certainly due to the better respect of the pin-hole model.

Influence of the CCD Resolution. With the third set-up, precision is increased by approximately 30% (Table 1 - Set-up 3). This increase can be attributed to the combination of a shorter focal length and a higher CCD resolution.

In terms of precision, the displacement measurements in the calibration board plane directions are comparable to the interferometric ones (Table 2). For this instrument, rotation around z cannot be measured. The vision-based measuring system also provides us simultaneously with accurate measurement of rotations.

Table 2: Interferometer specifications.

D.o.f	Interferometer specification
R_x	$1.7E - 5^\circ$
R_y	$1.7E - 5^\circ$
R_z	<i>non - measurable</i>
T_x	$1.15\mu m$
T_y	$1.15\mu m$
T_z	$0.35\mu m$

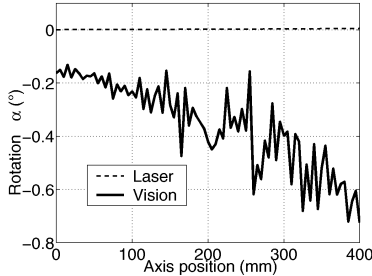


Figure 4: Rotation around x w.r.t position $z = 0$.

5.3 Trueness

First Measurement Configuration. An angular measurement bias can be observed on figures 4, 5. Translation measurement bias in x and y directions remain of small amplitude (figures 6, 7, 8), with an order of $0.01mm$. Their quantification is however quite delicate because of the previously underlined identification problem.

Influence of Calibration Board Size. Increasing pose estimation sensitivity to rotations, by modifying calibration board size, lowers significantly measurement bias. For the axis positions where the second calibration board can be observed, measurement bias is reduced by a factor 3.

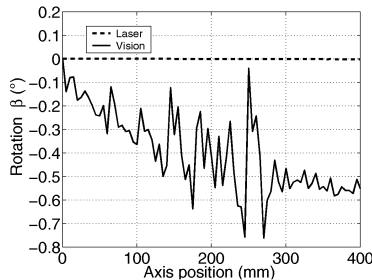


Figure 5: Rotation around y w.r.t position $z = 0$.

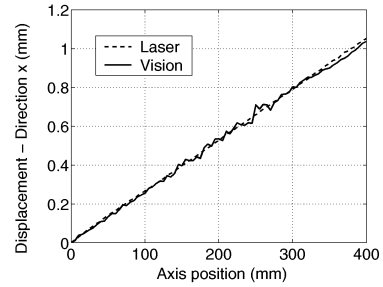


Figure 6: Translation along the x axis in the interferometer coordinate frame - Reference $z = 0$.

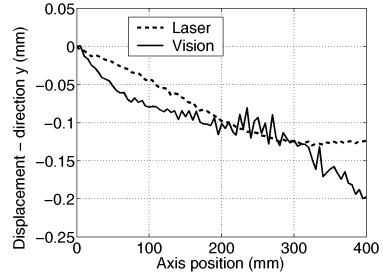


Figure 7: Translation along the y axis in the interferometer coordinate frame - Reference $z = 0$.

Influence of the Focal Length and CCD Resolution. The measurements with set-ups 2 & 3 have been achieved without the interferometer. The bias estimation procedure cannot therefore be applied. However, since the axis repeatability is very high, presence of bias can be evaluated by the amplitude of the measured angular variations. In the second measurement set-up, the use of a $8mm$ lens leads to angular variations comparable to the variations previously measured with the interferometer. Trueness seems therefore sharply increased with the use of this lens. Modification of the sensor resolution (Set-up 3) does not modify significantly the measurement bias.

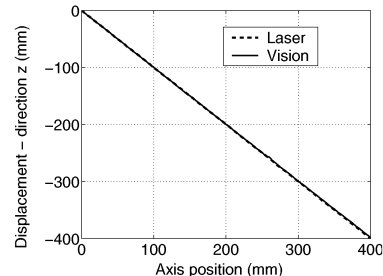


Figure 8: Translation along the z axis in the interferometer coordinate frame - Reference $z = 0$.

6 Conclusion

In this paper, a measuring system for parallel machine-tool calibration is experimentally evaluated. Composed of a single camera and screen-displayed calibration boards, the system is low-cost, easy to use, and the pose measurement enables one to perform calibration using IKM. Precision in the order of $1\mu\text{m}$ for 2 translations and $1E-3^\circ$ for the 3 rotations have been estimated for a displacement of 400mm . These specifications may be improved by the use of now available higher resolution CCD sensors, and by the introduction of a second camera to improve measurement performance on the third translation measurement. Following to this experimental evaluation, the study will be pursued by determining the calibration gain provided using this measuring system.

References

- [1] Leica Geosystems AG. Leica laser tracker system, 1999.
- [2] R. Bernhardt and S.L. Albright. *Robot Calibration*. Chapman and Hall, 1993.
- [3] S. Besnard and W. Khalil. Calibration of parallel robots using two inclinometers. In *Proc. Of the IEEE Int. Conf. On Rob. and Autom.*, pages 1758–1763, Detroit, Michigan, 1999.
- [4] B.C. Bouzgarrou. *Conception et Modélisation d'une machine-outil à architecture hybride pour l'UTGV*. PhD thesis, Université Blaise Pascal - Clermont II, Clermont-Ferrand, december 2001.
- [5] O. Company, F. Pierrot, F. Launay, and C. Fioroni. Modeling and preliminary design issues of a 3-axis parallel machine-tool. In *Proceedings of PKM'00*, pages 14–23, Ann-Harbor, 2000.
- [6] J.F. Curtino, D.E. Schinstock, and M.J. Prather. Three-dimensional metrology frame for precision applications. *Precision Engineering*, 23:103–112, 1999.
- [7] D. Daney. Self calibration of Gough platform using leg mobility constraints. In *Proceedings of the tenth world congress on the theory of machine and mechanisms*, pages 104–109, Oulu, 1999. IFToMM, Oulu University Press.
- [8] D. Daney. *Etalonnage Géométrique Des Robots Parallèles*. PhD thesis, Université de Nice - Sophia Antipolis, 2000.
- [9] M. Dhome, M. Richetin, J.T. Lapreste, and G. Rives. Determination of the attitude of 3-D objects from a single perspective view. *IEEE Transactions on Pattern Analysis and Machine Intelligence*, 11(12):1265–1278, 1989.
- [10] O. Faugeras. *Three-dimensional Computer Vision : A Geometric Viewpoint*. The MIT Press, 1993. ISBN 0-262-06158-9.
- [11] G. Fried, K. Djouani, Y. Amirat, and C. François. *A 3-D Sensor for Parallel Robot Calibration. A Parameter Perturbation Analysis*, pages 451–460. J. Lenarcic and V. Parenti-Castelli, 1996.
- [12] R. Horaud and O. Monga. *Vision Par Ordinateur - Outils Fondamentaux*. Hermès, Paris, 1993. ISBN 2-86601-370-0.
- [13] ISO. Iso 5725-1:1994 : Accuracy (trueness and precision) of measurement methods and results - part 1: General principles and definitions, 1994.
- [14] B.C. Jiang, R. Duraisamy, G. Wiens, and J.T. Black. Robot metrology using two kinds of measurement equipment. *Journal of Intelligent Manufacturing*, 8:137–146, 1997.
- [15] W. Khalil and S. Besnard. Self calibration of Stewart-Gough parallel robots without extra sensors. *IEEE Transactions on Robotics and Automation*, pages 1758–1763, 1999.
- [16] W. Khalil and E. Dombre. *Modélisation, Identification et Commande des Robots*. Hermès, 1999.
- [17] Y. Koseki, T. Arai, K. Sugimoto, T. Takatuji, and M. Goto. Design and accuracy evaluation of high-speed and high-precision parallel mechanism. In *Proceedings of the 1998 International Conference on Robotics and Automation*, volume 3, pages 1340–1345, Leuven, 1998.
- [18] JM. Lavest, M. Viala, and M. Dhome. Do we really need an accurate calibration pattern to achieve a reliable camera calibration. In *Proceedings of ECCV98*, pages 158–174, Freiburg, 1998.
- [19] O. Masory and Y. Jiahua. Measurement of pose repeatability of Stewart platform. *Journal of Robotic Systems*, 12(12):821–832, 1995.
- [20] J. Richalet. *Pratique de L'identification*. Hermès, 1998.
- [21] T. Schmitz and J. Ziegert. A new sensor for the micrometre-level measurement of three-dimensional, dynamic contours. *Measurement Science Technology*, 10:51–62, 1999.
- [22] H. Zhuang, O. Masory, and J. Yan. Kinematic calibration of a Stewart platform using pose measurements obtained by a single theodolite. In *IEEE Conf. On Intelligent Robots and Systems*, pages 329–334, Pittsburgh, 1995.
- [23] H. Zhuang and Z.S. Roth. Method for kinematic calibration of Stewart platforms. *Journal of Robotic Systems*, 10(3):391–405, 1993.
- [24] H. Zhuang, J. Yan, and O. Masory. Calibration of Stewart platforms and other parallel manipulators by minimizing inverse kinematic residuals. *Journal of robotic systems*, 15(7):395–405, 1998.
- [25] H. Zou and L. Notash. Discussions on the camera-aided calibration of parallel manipulators. In *Proceedings of the 2001 CCToMM Symposium on Mechanisms, Machines, and Mechatronic*, Saint-Hubert, 2001.